Supporting Information for

# Impact of Steric Effects on the Statistical Probability Factor in Triplet-Triplet Annihilation Upconversion

*Lukas Naimovičius, Simon K. Zhang, Andrew B. Pun**

Department of Chemistry and Biochemistry, University of California San Diego, 92093 La Jolla, CA, USA

*E-mail: abpun@ucsd.edu

## S1 General Considerations

All reagents/solvents were purchased from Sigma-Aldrich®, TCI America®, and VWR International®, and were used as received without further purification. Anhydrous solvents were obtained from a Schlenk manifold with purification columns packed with activated alumina and supported copper catalyst (Glass Contour, Irvine, CA). All reactions were carried out under nitrogen unless otherwise noted. Reactions and sample preparations requiring an inert atmosphere were carried out under nitrogen using standard Schlenk techniques or in a nitrogen-filled glovebox. $^{1}$H -NMR spectra were recorded on a 400 MHz Jeol ECZ spectrometer and $^{13}$C -NMR spectra were obtained on a 400 MHz Varian spectrometer. $^{1}$H and $^{13}$C chemical shifts (δ) are reported in ppm relative to the residual solvent signal ($CDCl_3$: 7.26 ppm for $^{1}$H NMR and 77.16 for $^{13}$C NMR). Standard abbreviations indicating multiplicity were used as follows: s (singlet), b (broad), d (doublet), t (triplet), q (quartet), m (multiplet), dd (doublet of doublets) and dt (doublet of triplets).

# S2 Synthetic Procedures

**DPP-Th**[1] was synthesized according to literature. [1] Synthesis of **DPP$_S$-Th**, **DPP-2*t*Bu-Th**, and **DPP$_S$-2*t*Bu-Th** was adapted from literature.[1]

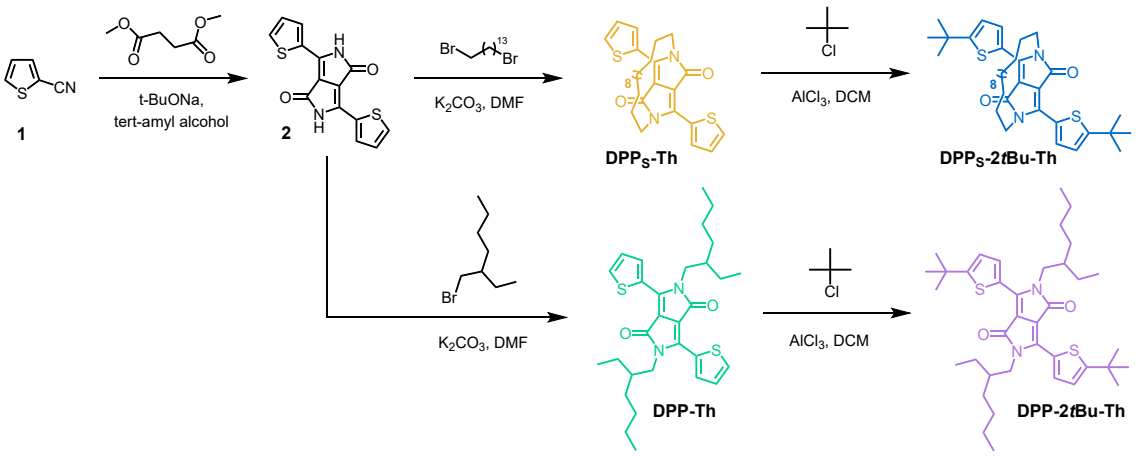


**Scheme S1**: Synthetic routes for DPP compounds.

## 3,6-di(thiophen-2-yl)-2,5-dihydropyrrolo[3,4-c]pyrrole-1,4-dione (2)

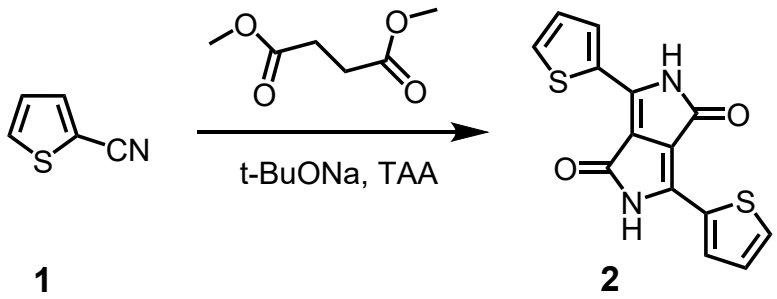


**1** **2**

In a three-neck round-bottom flask (RBF) with a magnetic stirring bar, sodium tert-butoxide (t-BuONa) (10.56 g, 109.9 mmol, 1.2 eq.) and tert-amyl alcohol (TAA) (200 ml) were added. The vessel was evacuated and backfilled with $N_2$ (3 times). The contents were heated to 80°C for 2 h to fully dissolve sodium tert-butoxide. Compound **1** (10.00 g, 91.6 mmol, 1.0 eq.) was added to the RBF. Vacuum/$N_2$ cycled again three times. The contents of the flask were stirred at 80°C for 1 h. Dimethyl succinate (6.02 g, 41.2 mmol, 0.45 eq.) dissolved in tert-amyl alcohol (20 ml) was added to RBF, color change to dark red occurred. Vacuum/$N_2$ cycled again three times. The contents of the flask were stirred at 115°C for 24 h. After that time the flask was cooled down to RT and the crude was filtered and washed with hot water and methanol. Compound **2** was obtained as a dark red solid. Yield: 7.0 g, 65%. The compound was not able to be characterized due to poor solubility and used in the next step as is.

**DPP-Th**

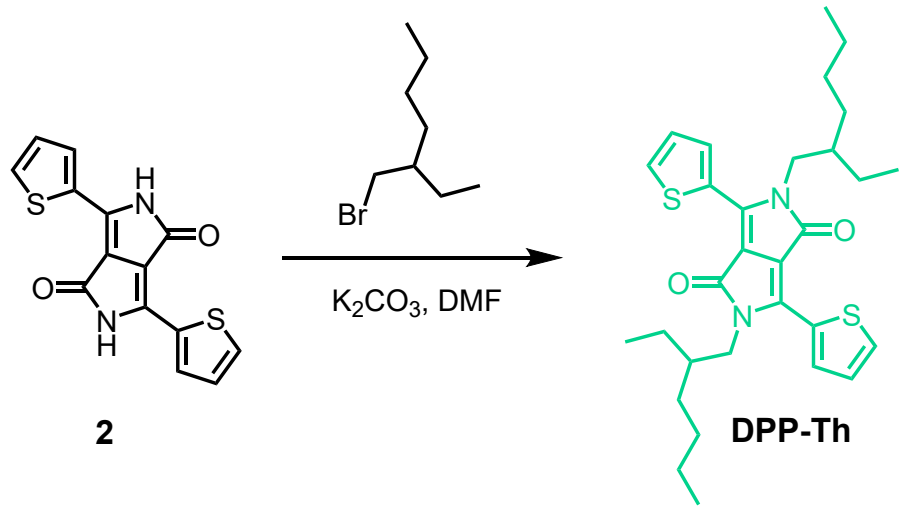


In a three-neck round-bottom flask with a magnetic stirring bar, compound **2** (6.00 g, 20.0 mmol, 1.0 eq.), potassium carbonate ($K_2CO_3$) (11.06 g, 80.0 mmol, 4.0 eq.), and dry DMF (160 ml) were added. The vessel was evacuated and backfilled with $N_2$ (3 times). The contents were heated to 120°C for 2 h. 2-ethylhexyl bromide (19.30 g, 100.0 mmol, 5.0 eq.) was added to the RBF. Vacuum/$N_2$ cycled again three times. The contents of the flask were stirred at 130°C for 72 h. After, the flask was cooled down to RT, contents were poured into water, organics extracted with DCM and washed with brine. All solvents were evaporated off. The residue was purified by column chromatography ($SiO_2$, hexane : DCM = 1 : 1). Again, all solvents were evaporated off. In the next step, the product was recrystallized by dissolving it in a vial in as little DCM as possible and then filling the vial with methanol. The contents were left for 12 h to recrystallize. Then, the crystals were filtered and dried under vacuum. The **DPP-Th** was obtained as red-purple crystals. Yield 1.70g, 16%. $^1$H NMR (400 MHz, $CDCl_3$) δ 8.89 (dd, 2H), 7.63 (dd, 2H), 7.29 (dd, 2H), 4.03 (d, 4H), 1.85 (m, 2H), 1.40-1.22 (b, 16H), 0.89-0.83 (m, 12H). $^{13}$C NMR (400 MHz, $CDCl_3$) δ 161.86, 140.53, 135.41, 130.66, 129.92, 128.54, 107.99, 45.93, 39.15, 30.28, 28.43, 23.59, 23.17, 14.14, 10.57.

**$DPP_S$-Th**

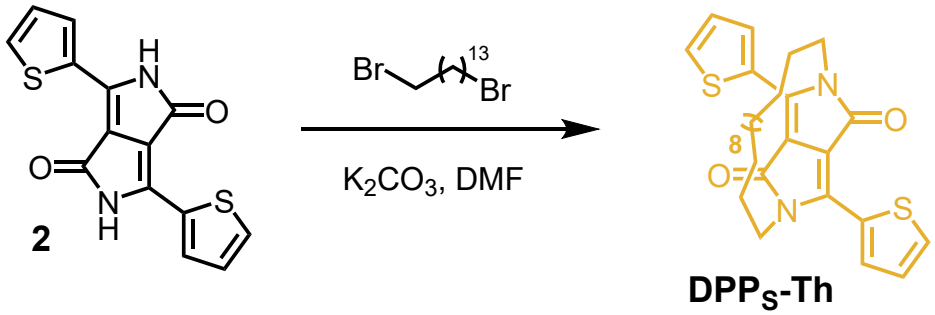


In a three-neck round-bottom flask with a magnetic stirring bar, compound **2** (1.00 g, 3.33 mmol, 1.0 eq.), potassium carbonate ($K_2CO_3$) (1.84 g, 13.32 mmol, 4.0 eq.), and dry DMF (120 ml) were added. The vessel was evacuated and backfilled with $N_2$ (3 times). The contents were heated to 120°C for 2 h. 1,14-dibromotetradecane (1.19 g, 3.33 mmol, 1.0 eq.) was added to the RBF. Vacuum/$N_2$ cycled again three times. The contents of the flask were stirred at 130°C for 40 h. After, the flask was cooled down to RT, contents were poured into water, organics extracted with DCM and washed with brine. All solvents were evaporated off. The residue was purified by column chromatography ($SiO_2$, DCM). Again, all solvents were evaporated off. In the next step, the product was recrystallized by dissolving it in a vial in as little DCM as possible and then filling the vial with methanol. The contents were left for 12 h to recrystallize. Then, the crystals were filtered and dried under vacuum. The **$DPP_S$-Th** was obtained as dark green crystals. Yield 0.214 g, 13%. $^1$H NMR (400 MHz, $CDCl_3$) δ 8.78 (dd, 2H), 7.63 (dd, 2H), 7.28 (dd, 2H), 4.46 (d, 2H), 3.99 (d, 2H), 1.85 (m, 2H), 1.40-1.22 (b, 16H), 0.89-0.83 (m, 12H). $^{13}$C NMR (400 MHz, $CDCl_3$) δ 162.09, 140.37, 134.93, 130.73, 130.07, 128.49, 108.47, 41.12, 29.20, 28.80, 27.76, 27.59, 26.93, 24.01.

**DPP-2*t*Bu-Th**

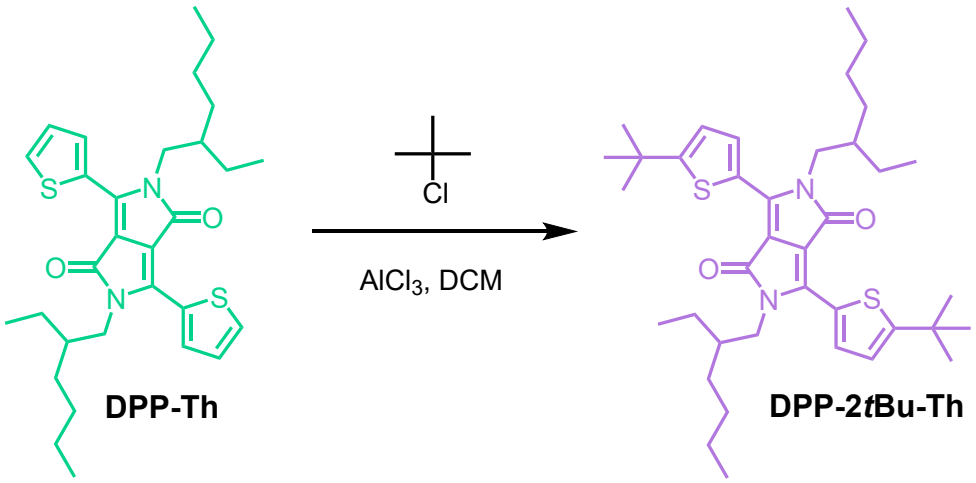


In a three-neck round-bottom flask with a magnetic stirring bar, **DPP-Th** (0.25 g, 0.48 mmol, 1.0 eq.), tertbutyl chloride (0.22 g, 2.40 mmol, 5.0 eq.), and DCM (17 ml) were added. The vessel was evacuated and backfilled with $N_2$ (3 times). Then, the flask was submerged in an ice-water bath. Aluminum trichloride ($AlCl_3$) (0.32 g, 2.40 mmol, 5.0 eq.) was added in two portions. Vacuum/$N_2$ cycled again three times. The contents were left to stir at RT for 48 h. After that time, the contents of the flask were stirred at 35°C for the additional 24 h. After, the reaction was quenched with ice, contents were poured into water, organics extracted with DCM and washed with brine. All solvents were evaporated off. The residue was purified by column chromatography ($SiO_2$, hexane : DCM = 1 : 1). Again, all solvents were evaporated off. In the next step, the product was recrystallized by dissolving it in a vial in as little DCM as possible and then filling the vial with methanol. The contents were left for 12 h to recrystallize. Then, the crystals were filtered and dried under vacuum. The **DPP-2*t*Bu-Th** was obtained as light red crystals. Yield 0.11 g, 35%. $^{1}$H NMR (400 MHz, $CDCl_3$) δ 8.74 (dd, 2H), 7.00 (dd, 2H), 4.01 (m, 4H), 1.85 (m, 2H), 1.44 (s, 18H), 1.36-1.24 (b, 16H), 0.90-0.83 (m, 12H). $^{13}$C NMR (400 MHz, $CDCl_3$) δ 163.94, 161.96, 140.36, 135.75, 127.00, 123.42, 107.46, 45.82, 39.34, 35.22, 32.78, 30.54, 28.77, 23.77, 23.21, 14.19, 10.71.

**$DPP_S$-2*t*Bu-Th**

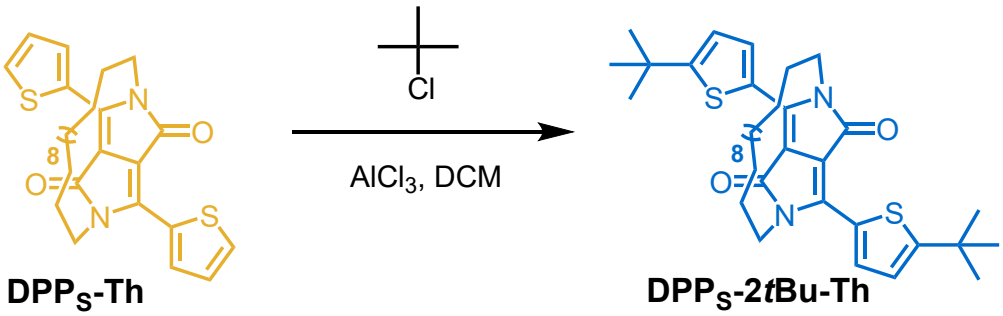


In a three-neck round-bottom flask with a magnetic stirring bar, **$DPP_S$-Th** (0.217 g, 0.44 mmol, 1.0 eq.), tertbutyl chloride (0.20 g, 2.20 mmol, 5.0 eq.), and DCM (14 ml) were added. The vessel was evacuated and backfilled with $N_2$ (3 times). Then, the flask was submerged in an ice-water bath. Aluminum trichloride ($AlCl_3$) (0.29 g, 2.20 mmol, 5.0 eq.) was added in two portions. Vacuum/$N_2$ cycled again three times. The contents were left to stir at RT for 72 h. After, the reaction was quenched with ice, contents were poured into water, organics extracted with DCM and washed with brine. All solvents were evaporated off. The residue was purified by column chromatography ($SiO_2$, hexane : DCM = 1 : 1). Again, all solvents were evaporated off. In the next step, the product was recrystallized by dissolving it in a vial in as little DCM as possible and then filling the vial with methanol. The contents were left for 12 h to recrystallize. Then, the crystals were filtered and dried under vacuum. The **$DPP_S$-2*t*Bu-Th** was obtained as dark red crystals. Yield 0.11 g, 43%. $^1$H NMR (400 MHz, $CDCl_3$) δ 8.65 (dd, 2H), 6.99 (dd, 2H), 4.44 (m, 2H), 4.01 (dd, 2H), 1.69 (m, 4H), 1.45 (s, 18H), 1.38-1.32 (b, 2H), 1.23-1.05 (m, 18H). $^{13}$C NMR (400 MHz, $CDCl_3$) δ 164.12, 162.19, 140.27, 135.29, 127.24, 123.37, 107.94, 41.09, 35.27, 32.43, 29.18, 28.97, 27.83, 27.71, 26.96, 24.08.

## S3 DFT Calculations

Molecular geometry as well as singlet and triplet state energies of the annihilators were modelled using the quantum chemistry program *ORCA*.[2] The DFT geometry optimization for DPP compounds was performed at the B3LYP/6-31G(d) level in vacuum.[3–5] Later, time-dependent density functional theory (TD-DFT) calculations were performed to extract singlet and triplet state energies.

DFT calculation data have been deposited in a multi-disciplinary repository Zenodo. The raw calculation output files are provided for transparency and reproducibility. Data can be accessed via DOI: 10.5281/zenodo.12692754.

## S4 MD Simulations

Molecular dynamics simulations were performed using Molecular Operating Environment (MOE) software.[6] Molecular structures were optimized using AMBER10:EHT forcefield, the intermolecular collisions were modelled in ambient conditions (300 K) by employing Nosé-Hoover-Andersen (NHA) simulation algorithm with a 2000 ps production range. The dielectric constant of 2.4 was introduced as an implicit solvent environment corresponding to toluene.

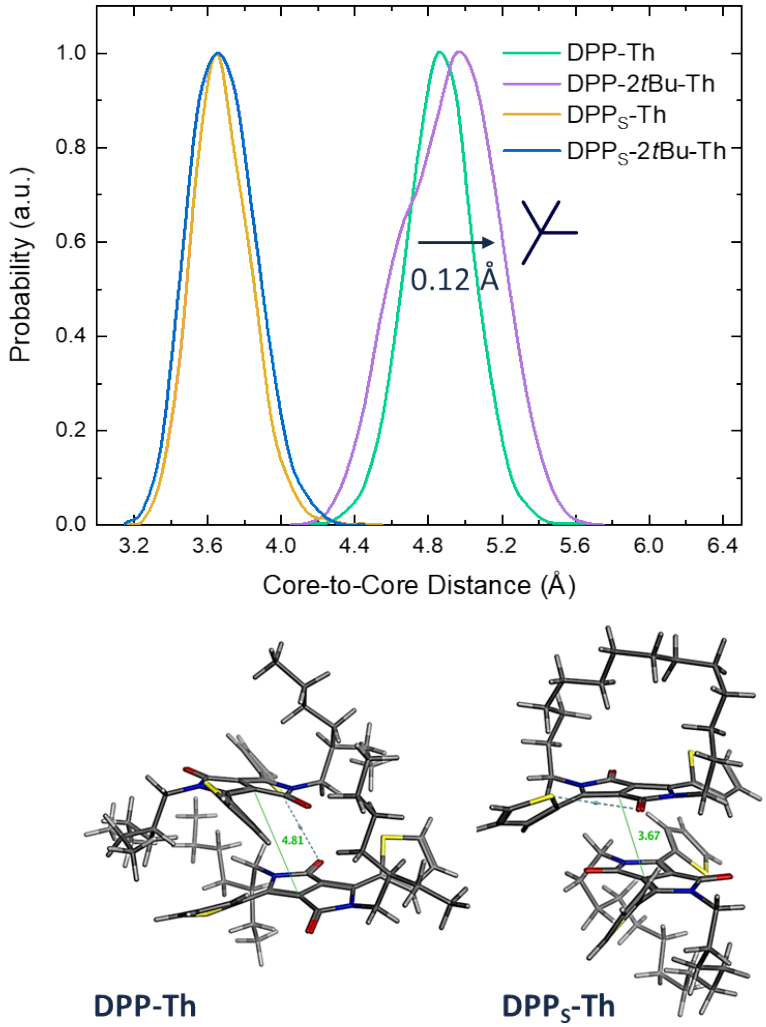


**Figure S1**: a) Distribution of intermolecular distance between the cores of DPP compounds during collision. Shift of 0.12 Å indicated due to *t*Bu moiety. A dielectric constant of 2.4 is employed in an implicit solvent model to correspond to toluene. b) Optimized collision structures for DPP-Th and $DPP_S$-Th. Core-to-Core distance is indicated in Å.

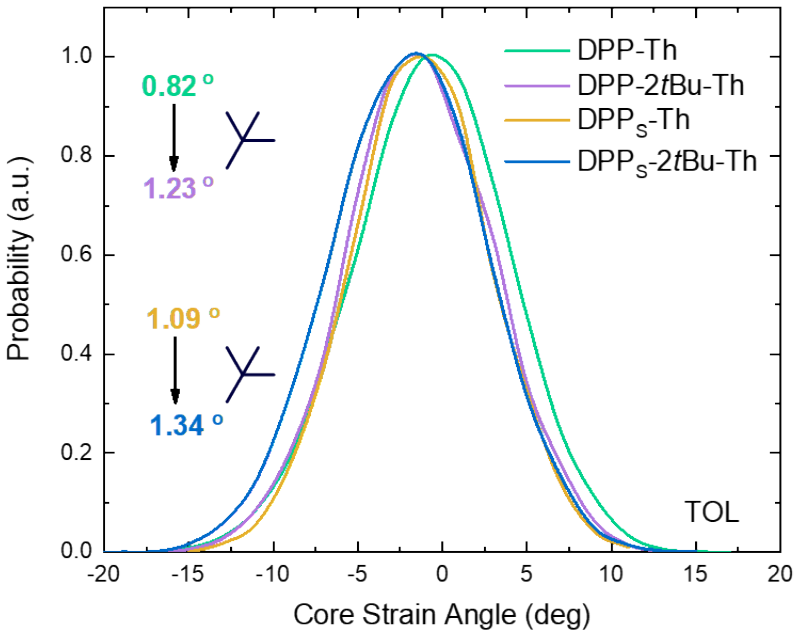


**Figure S2**: Core strain angle between the cores of DPP compounds during collision. Change in angle due to tert-butyl moiety indicated. A dielectric constant of 2.4 is employed in an implicit solvent model to correspond to toluene.

## S5 Optical Characterization

Solutions of DPP derivatives (1 mM to 26 mM) and $PdPc(OBu)_8$ (30 µM) were prepared from anhydrous toluene in a nitrogen glovebox ($H_2O$ and $O_2$ <0.1 ppm). Measurements performed in a sealed 2 mm fused quartz cuvette. Upconversion measurements were conducted with a 730 nm laser diode (HL7302MG) from Thorlabs® powered by a Keithley 2400 SourceMeter®. The laser was focused to the area of 4754 µm$^2$. All UC spectra were measured with an Ocean HDX miniature spectrometer by Ocean Insight®. All optical elements were purchased from Thorlabs®. A 700 nm short-pass filter (FESH0700) was utilized for UC measurements. For UC threshold measurements, a variety of ND filters (NEK01) were used on a rotary lens holder. Absorption measurements were collected on an Agilent Cary 60 spectrophotometer. All measurement samples were prepared under air using commercial toluene and cuvettes were sealed with Teflon caps. Photoluminescence spectra were taken with a 515nm laser from Thorlabs®.

Photoluminescence quantum yield ($\Phi_{PL}$) measurements were performed on a Hamamatsu Quantaurus-QY C1134 with the corresponding long-stem quartz cuvette and commercial toluene. Excitation wavelength was scanned from 400 to 500 nm with a 10 nm step, average values of $\Phi_{PL}$ reported.

## S6 Upconversion Quantum Yield

Relative UC quantum yield was determined following the method reported elsewhere.[7–9] Indocyanine Green was selected as the reference due to its similar absorption range to PdPc. The photoluminescence quantum yield of indocyanine green was reported to be $\Phi_R$ = 14% in ethanol.[10] UC and reference samples were excited with a 730 nm laser under identical configuration and excitation intensity. A 750 nm long-pass filter was used for the reference and a 700 nm short-pass filter for the measurement of the UC samples. The following equation was employed to calculate relative $\Phi_{UC}$:[11]

$$\Phi_S = \Phi_R\left(\frac{I_S}{I_R}\right)\left(\frac{1-10^{-A_R}}{1-10^{-A_S}}\right)\left(\frac{n_S}{n_R}\right)^2$$

where Φ, I, A, and n represent the quantum yield, integrated UC or PL intensity, absorbance, and refractive index of the solvent. The subscripts S and R indicate the parameters of sample and reference systems.

**Table S1** Main parameters of the relative $\Phi_{UC}$ measurement for DPP:PdPc UC solutions at optimal 26 mM and 30 μM concentrations in toluene, respectively.

| Sample | A (OD) | Normalized Integ. Int. | $\Phi_{PL}$ (%) | n | $\Phi_{UC}$ (%)[a] |
|---|---|---|---|---|---|
| Indocyanine Green | 0.118 | 1.000 | 14.00 | 1.3614 | - |
| $DPP_S$-Th | 0.219 | 0.409 | - | 1.4968 | 4.18 |
| DPP-Th | | 0.297 | | | 3.03 |
| $DPP_S$-2*t*Bu-Th | | 0.282 | | | 2.88 |
| DPP-2*t*Bu-Th | | 0.261 | | | 2.66 |

[a] External UC quantum yield indicated.

## S7 Reabsorption Correction

To determine the internal UC quantum yield ($\Phi_{UC,g}$), the external UC quantum yield should be corrected for self-reabsorption. The 700 nm short-pass filter used for the UC measurements cuts off a small portion of the UC emission, which is also required to be corrected. To determine the internal UC quantum yield, the emissions of the UC samples were measured upon excitation with both 730 nm (UC) and 515 nm light (PL) to correct for self-reabsorption and short-pass filter effect (Fig. S3). The plots were fit to the corresponding first vibrational peak. The ratio between integrated internal and external UC emission was calculated (Table S2) and employed to determine the internal UC quantum yield.

**Table S2**: Reabsorption ratios for DPP annihilators at 26 mM in DPP:PdPc UC solutions.

| Compound | Reabsorption ratio |
|---|---|
| $DPP_S$-Th | 1.146 |
| DPP-Th | 1.159 |
| $DPP_S$-2*t*Bu-Th | 1.174 |
| DPP-2*t*Bu-Th | 1.162 |

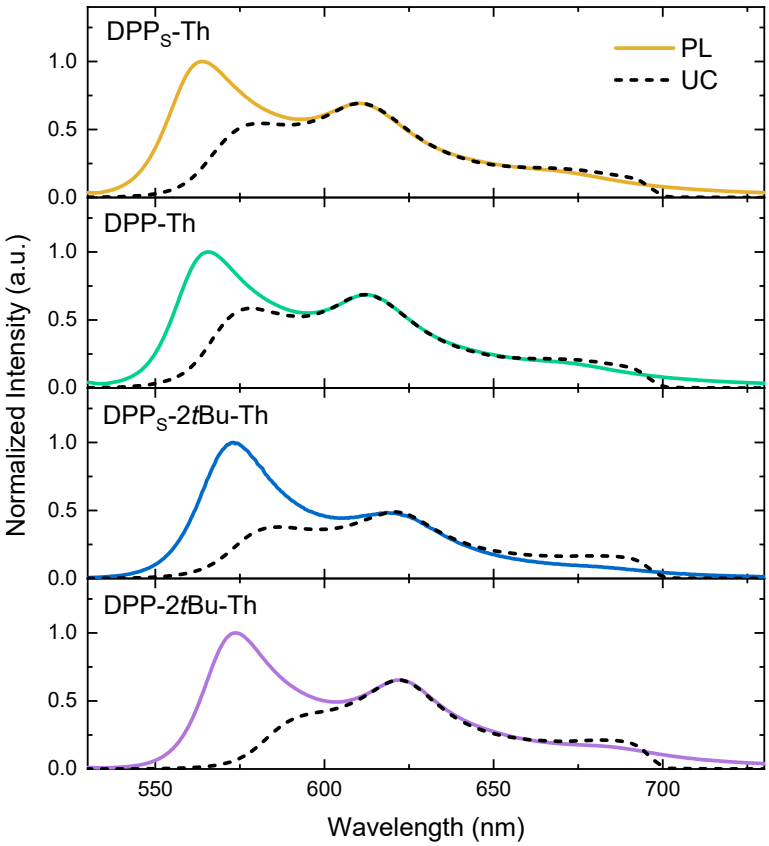


**Figure S3**: Self-reabsorption correction of UC emission for DPP:PdPc UC solutions in toluene at 26 mM and 30 µM, respectively. Samples were excited with either 515 nm (PL, solid line) or 730 nm (UC, dashed line) laser.

## S8 Upconversion Threshold

To determine UC threshold and maximum achievable UC quantum yield ($\Phi^{\infty}_{UC,g}$) for UC systems, neutral density (ND) filters were placed in front of the excitation source (730 nm laser diode) to gradually change the excitation power density. Laser spot size was determined to be 4754 µm$^2$.

To determine the maximum achievable UC quantum yield ($\Phi^{\infty}_{UC,g}$) of the UC systems and their threshold intensities ($I_{th}$), the $\Phi_{UC,g}$ dependence on excitation power density was investigated. This data was fit according to the following equation by Murakami et al.[12]

$$\Phi_{UC,g} = \Phi_{UC,g}^{\infty}\left(1 + \frac{1 - \sqrt{1 + 4\left(I_{ex}/I_{th}\right)}}{2\left(I_{ex}/I_{th}\right)}\right)$$

The method allows to estimate the $\Phi^{\infty}_{UC,g}$ as the TTA quantum yield ($\Phi_{TTA}$) approaches unity at high $I_{ex}$. $\Phi^{\infty}_{UC,g}$ is then utilized for the estimation of the statistical probability factor (f). $I_{th}$ is defined as the $I_{ex}$ where $\Phi^{\infty}_{UC,g}$ reaches 38.2% of its maximum value.[13]

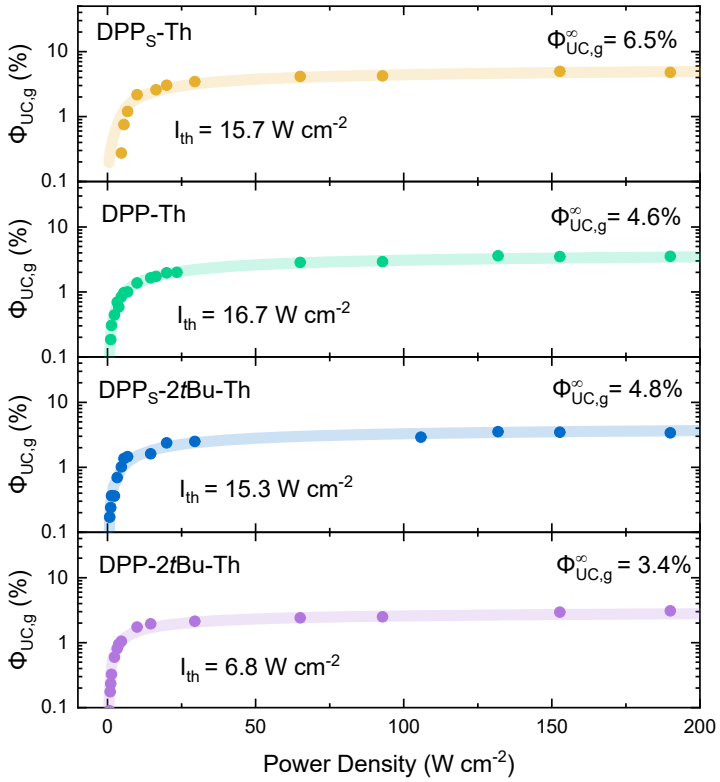


**Figure S4**: UC quantum yield dependence on excitation power density for DPP:PdPc UC solutions prepared in toluene at optimal concentrations of 26 mM and 30 µM, respectively. UC threshold and maximum UC quantum yield indicated.

## S9 Triplet Energy Transfer

Triplet energy transfer quantum yield ($\Phi_{TET}$) for each studied DPP:PdPc UC system was evaluated by employing a Stern-Volmer relationship of sensitizer (PdPc) phosphoresence (P) as a function of annihilator concentration. The P intensity of the sensitizer (I) was measured at different annihilator (acceptor) concentrations ([c]) while sensitizer (donor) concentration remained constant (30 μM). The rate of TET ($k_{TET}$) was determined by employing the Stern-Volmer relation:

$$\frac{I_0}{I} = 1 + k_{TET}\tau_0[c]$$

Where $I_0$ is intensity of unquenched sensitizer P, and $\tau_0$ is the P lifetime of our sensitizer (3.04 μs).[14]

$\Phi_{TET}$ was estimated using the following equation:

$$\Phi_{TET} = 1 - \frac{\Phi_{P(UC)}}{\Phi_P}$$

Where $\Phi_{P(UC)}$ is the phosphorescence quantum yield of the sensitizer in DPP:PdPc UC solution, and $\Phi_P$ is the quantum yield of the sensitizer phosphorescence in the absence of annihilator (77%).[15]

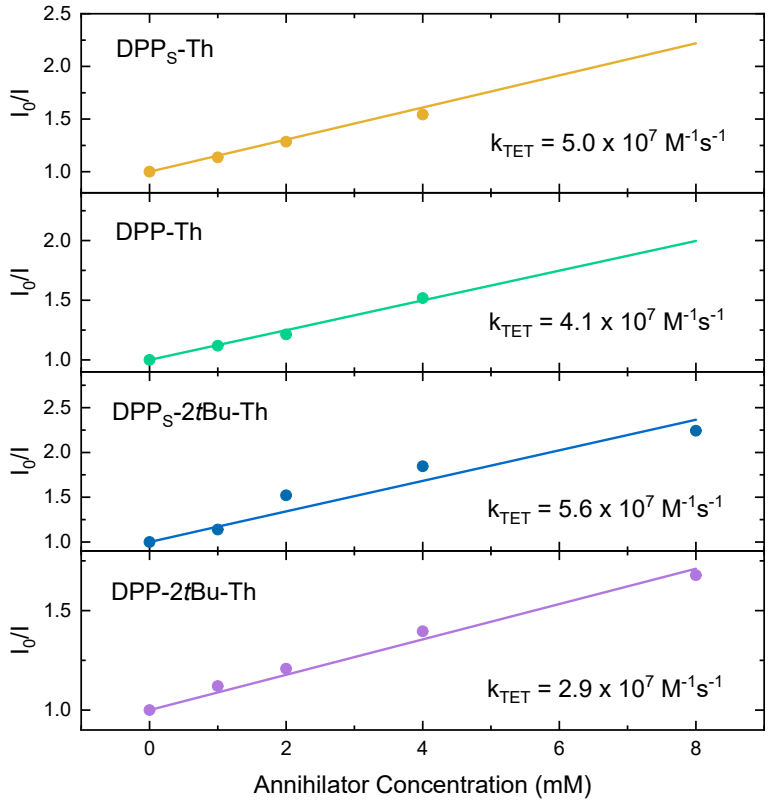


**Figure S5**: Integrated phosphorescence intensity ratio of 30 µM PdPc in toluene as a function of concentration of annihilators. Excited with a 730 nm laser diode. 900 nm long pass filter used.

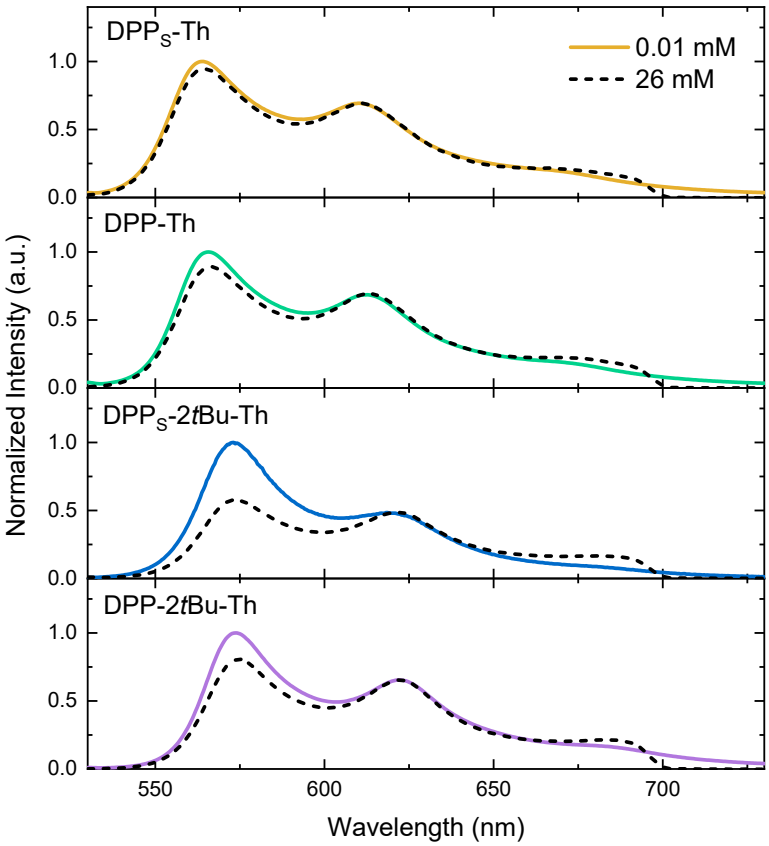


**Figure S6**: Comparison of PL emission between DPP:PdPc solutions in toluene at 26 mM (dashed line) and 30 µM, respectively, and DPP solutions at 0.01 mM (solid line). Samples were excited with 515 nm laser. A 700 nm short pass filter used for the measurement of the DPP:PdPc solutions.

## S10 Statistical Probability Factor

Statistical probability factors (*f*) for each compound were determined using the following equation:

$$\Phi_{UC,g}^{\infty} = \frac{1}{2} f \Phi_{ISC} \Phi_{TET} \Phi_{TTA} \Phi_{PL}$$

$\Phi_{ISC}$ is unity for PdPc. Assuming infinite power, $\Phi_{TTA}$ is 100%.[16]

## S11 NMR Spectra

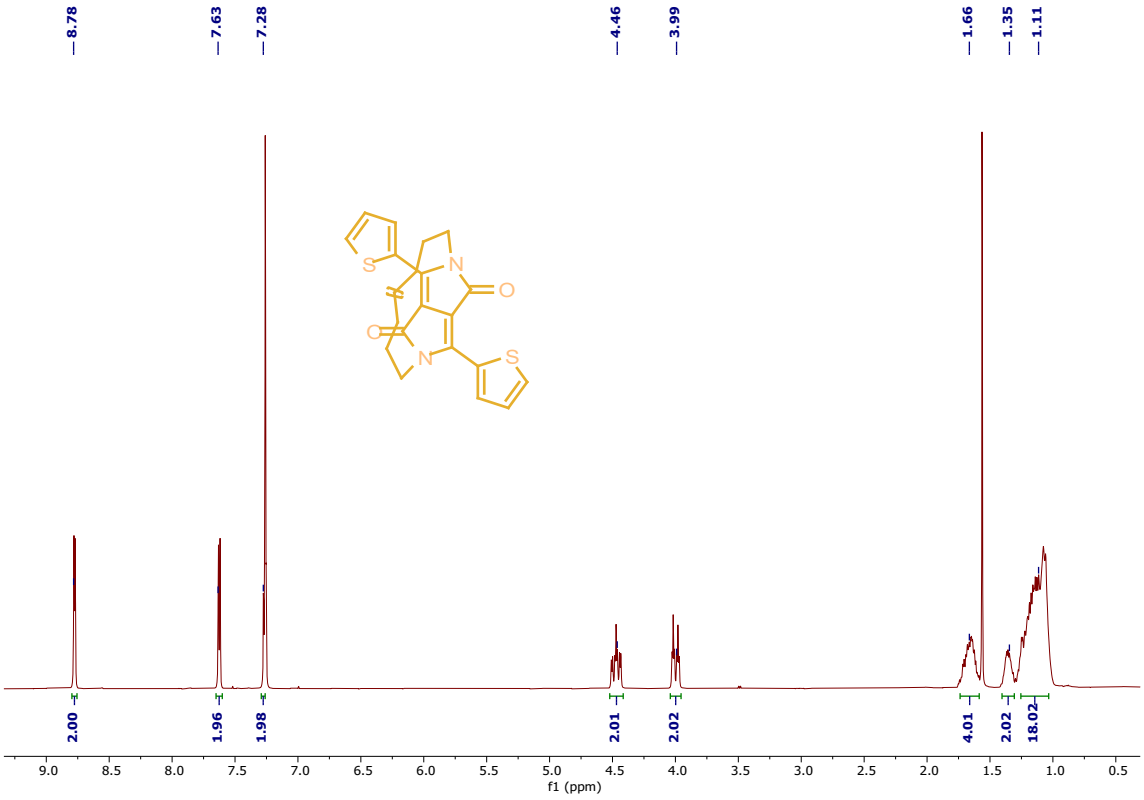


$^1$H NMR Spectrum of **DPP$_S$-Th**

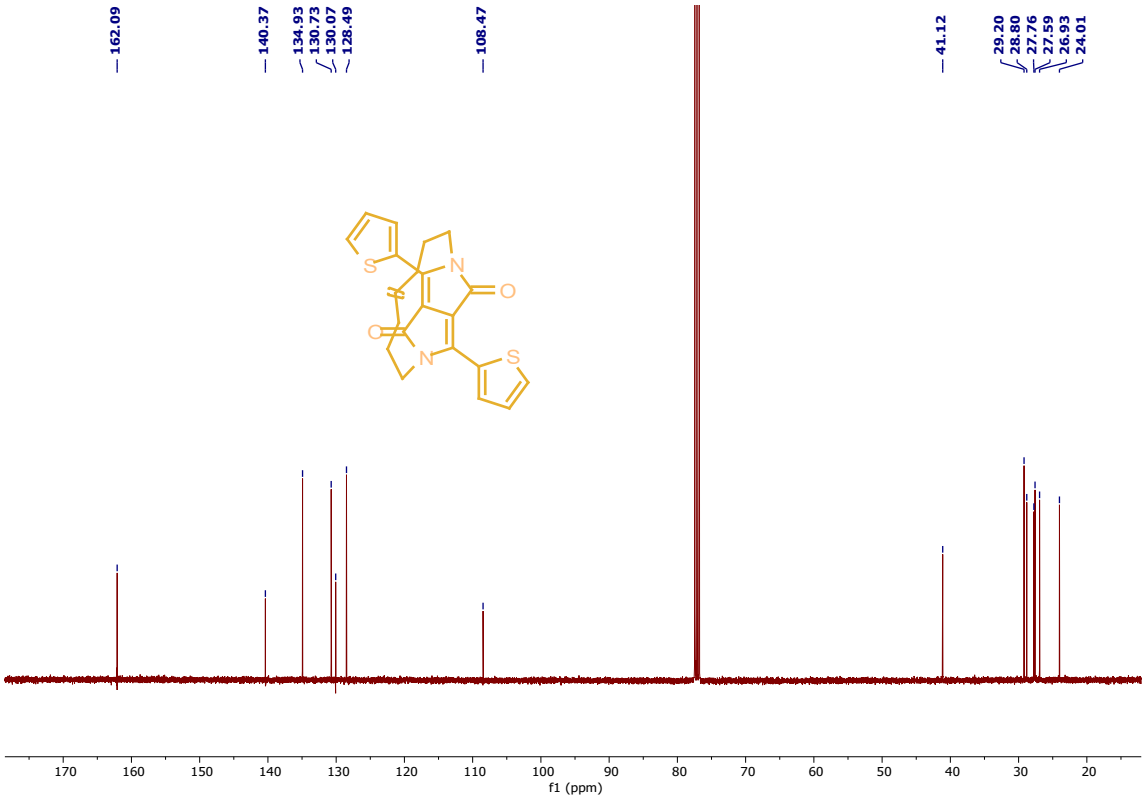


$^{13}$C NMR Spectrum of **DPP$_S$-Th**

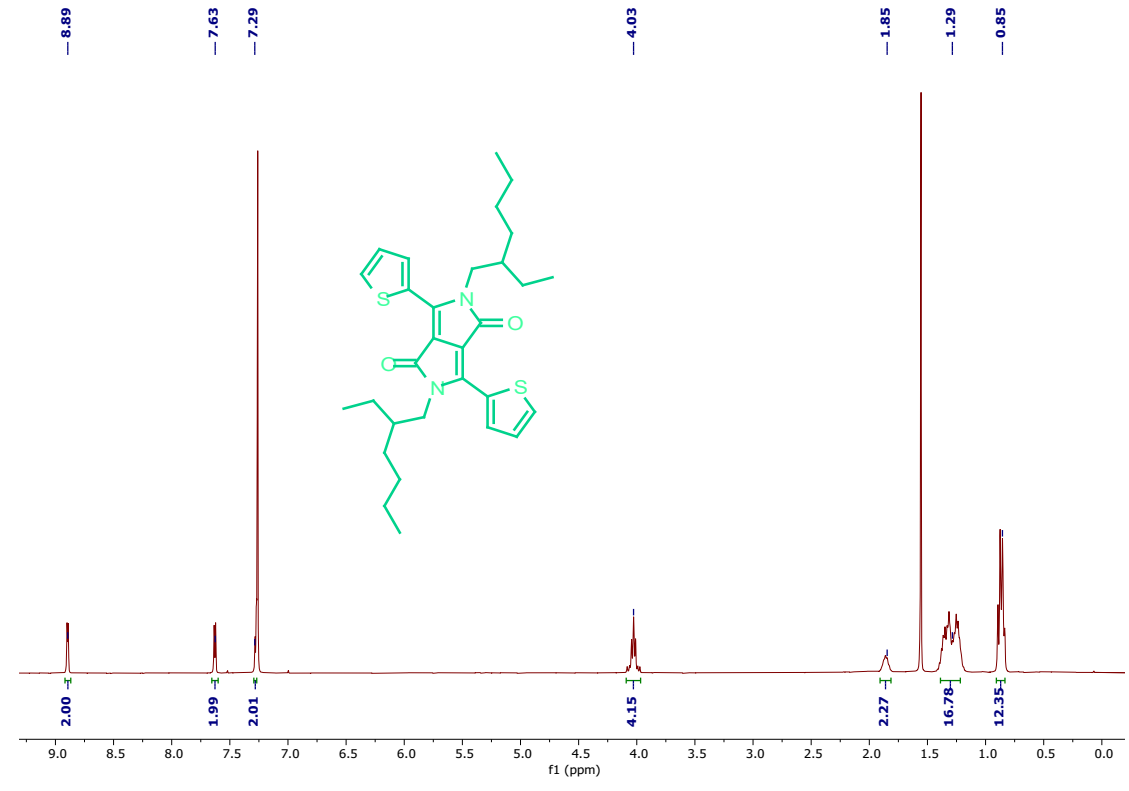


$^{1}$H NMR Spectrum of **DPP-Th**

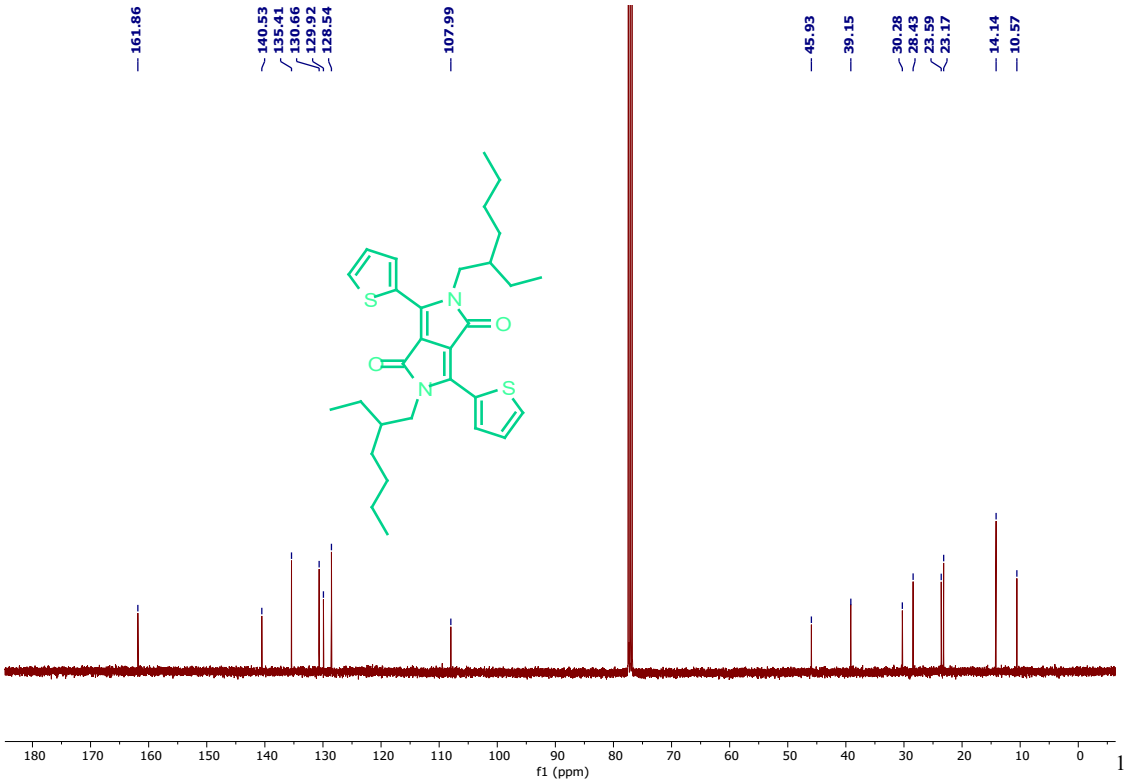




C NMR Spectrum of **DPP-Th**

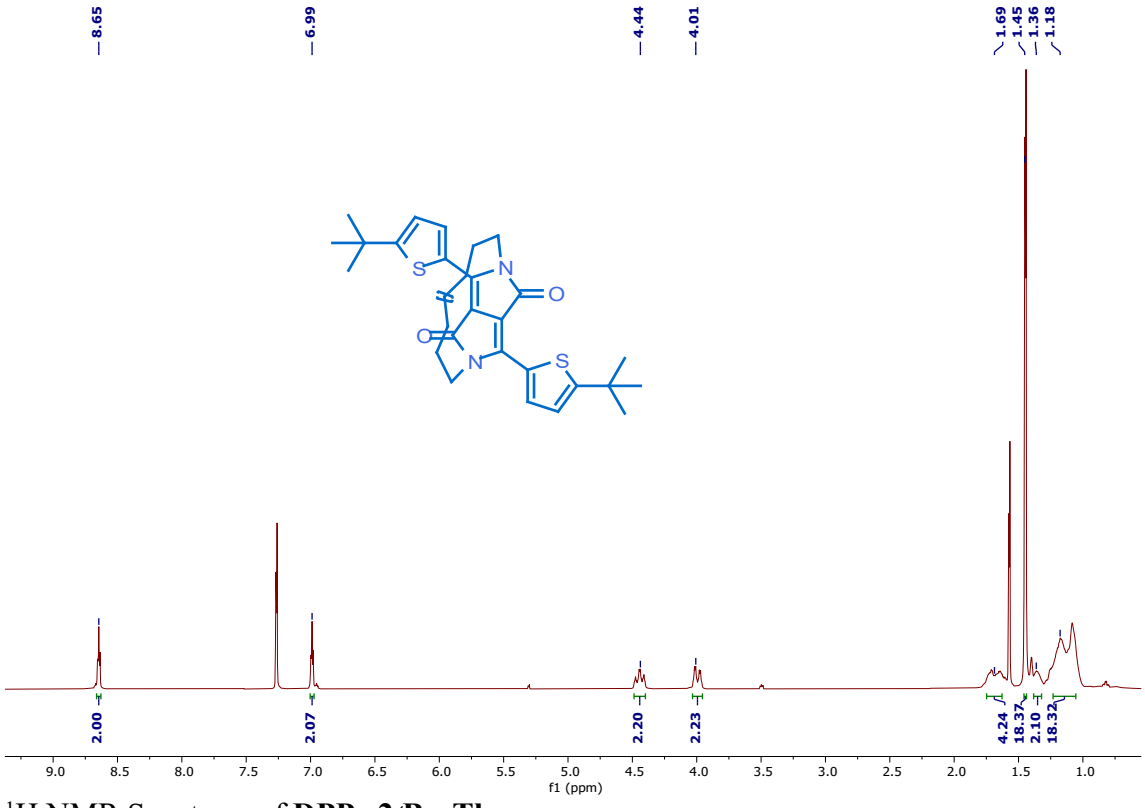


$^{1}$H NMR Spectrum of **DPP$_S$-2*t*Bu-Th**

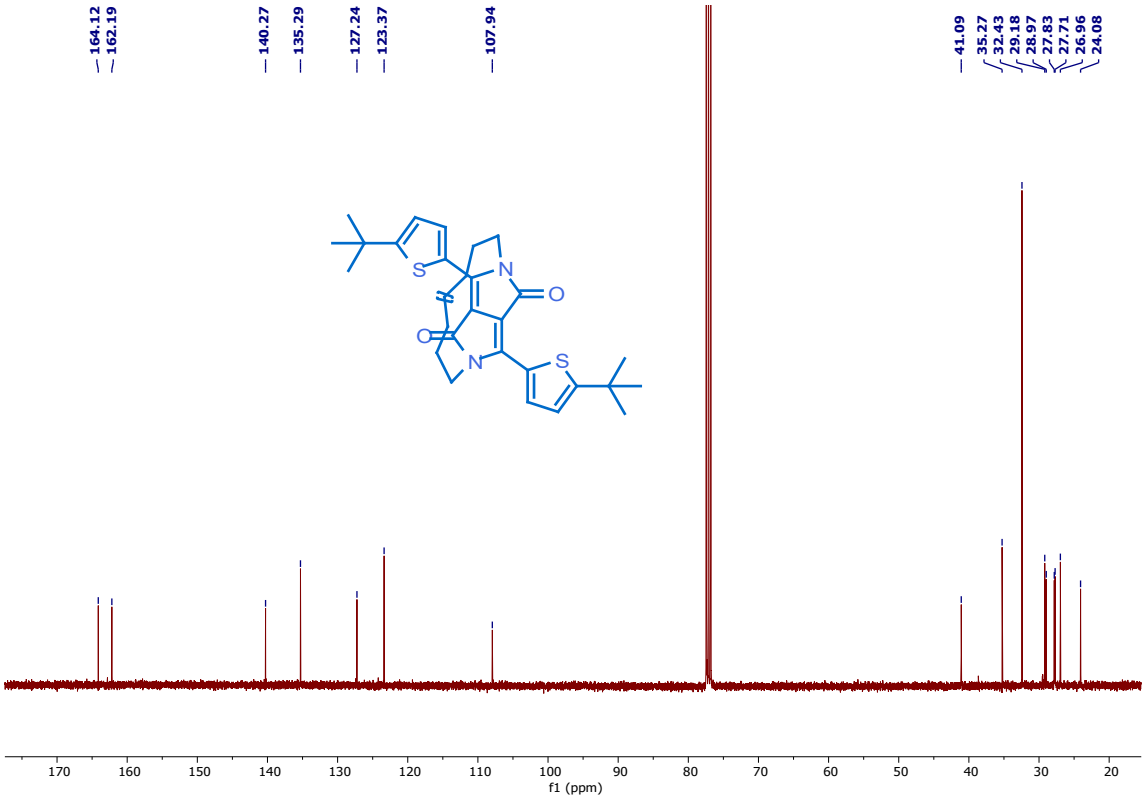


$^{13}$C NMR Spectrum of **DPP$_S$-2*t*Bu-Th**

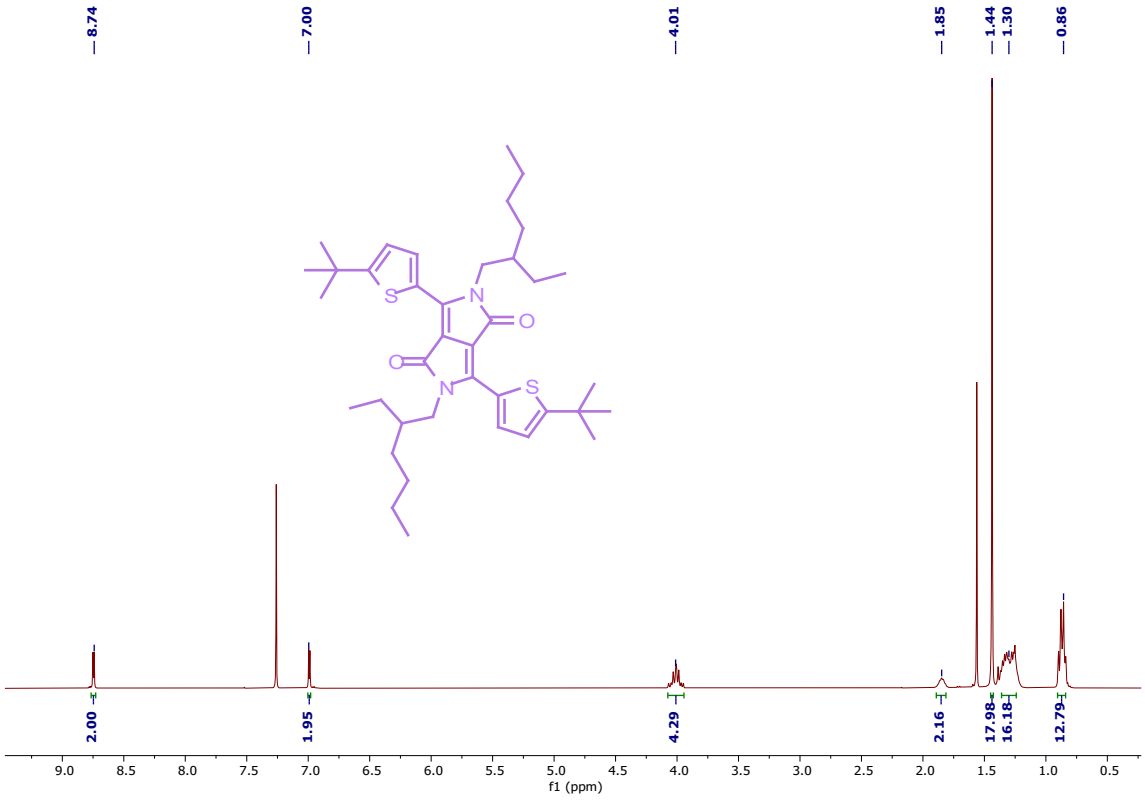


$^{1}$H NMR Spectrum of **DPP-2*t*Bu-Th**

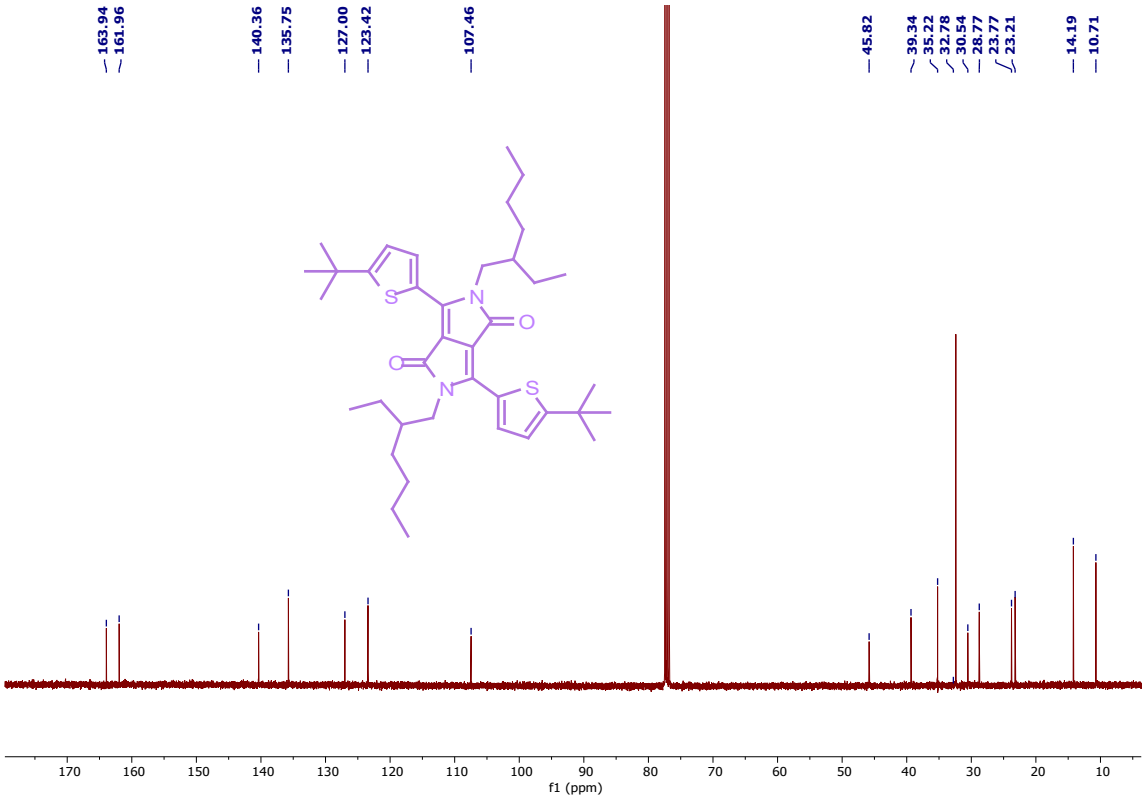


$^{13}$C NMR Spectrum of **DPP-2*t*Bu-Th**

## S12 References


1 J. Yu, B. Zhao, X. Nie, B. Zhou, Y. Li, J. Hai, E. Zhu, L. Bian, H. Wu and W. Tang, *New J. Chem.*, 2015, **39**, 2248–2255.

2 F. Neese, *Wiley Interdiscip. Rev. Comput. Mol. Sci.*, 2012, **2**, 73–78.

3 A. D. Becke, *J. Chem. Phys.*, 1993, **98**, 5648–5652.

4 P. J. Stephens, F. J. Devlin, C. F. Chabalowski and M. J. Frisch, *J. Phys. Chem.*, 1994, **98**, 11623–11627.

5 W. J. Hehre, R. Ditchfield and J. A. Pople, *J. Chem. Phys.*, 1972, **56**, 2257–2261.

6 2022.02 Chemical Computing Group ULC Molecular Operating Environment (MOE), 2024.

7 S. Hoseinkhani, R. Tubino, F. Meinardi and A. Monguzzi, *Phys. Chem. Chem. Phys*, 2015, **17**, 4020–4024.

8 N. Yanai, K. Suzuki, T. Ogawa, Y. Sasaki, N. Harada and N. Kimizuka, *J. Phys. Chem. A*, 2019, **123**, 10197–10203.

9 L. Naimovičius, E. Radiunas, M. Dapkevičius, P. Bharmoria, K. Moth-Poulsen and K. Kazlauskas, *J. Mater. Chem. C*, 2023, **11**, 14826–14832.

10 E. D. Cosco, I. Lim and E. M. Sletten, *ChemPhotoChem*, 2021, **5**, 727–734.

11 L. Naimovičius, E. Radiunas, M. Dapkevičius, P. Bharmoria, K. Moth-Poulsen and K. Kazlauskas, *J. Mater. Chem. C*, 2023, **11**, 14826–14832.

12 Y. Murakami and K. Kamada, *Phys. Chem. Chem. Phys.*, 2021, **23**, 18268–18282.

13 F. Edhborg, A. Olesund and B. Albinsson, *Photochem. Photobiol. Sci.,* 2022, **21**, 1143–1158.

14 A. V Soldatova, J. Kim, C. Rizzoli, M. E. Kenney, M. A. J. Rodgers, A. Rosa and G. Ricciardi, *Inorg. Chem.*, 2011, **50**, 1135–1149.

15 B. D. Rihter, M. E. Kenney, W. E. Ford and M. A. J. Rodgers, *J. Am. Chem. Soc.*, 1990, **112**, 8064–8070.

16 E. Radiunas, S. Raišys, S. Juršėnas, A. Jozeliūnaitė, T. Javorskis, U. Šinkevičiūtė, E. Orentas and K. Kazlauskas, *J. Mater. Chem. C*, 2020, **8**, 5525–5534.